A High Rock Cut Stabilization in Muscat City, Oman

Tahir M. Hayat, *Vice President, Geotechnical and Geonvironmental Engineering Division, NESPAK , Lahore, Pakistan; email: tmhayat786@yahoo.com*
Tariq J. Bhatti, *Chief Geologist, Geotechnical and Geonvironmental Engineering Division, NESPAK , Lahore, Pakistan; email: tariqjb@gmail.com*
Robert Goldsmith, *Technical Principal- Engineering Geology, Snowy Mountains Engineering Corporation (SMEC), Australia; email: Robert.Goldsmith@smec.com*

ABSTRACT: *A large road box cut was constructed in hilly terrain of Muscat city, Oman, in an area underlain by the geologically complex Sahtan and Mahil formations comprising of limestone, dolomite, sandstone and siltstone with interbedded soft calcareous mudstone. The rockmass contains a large number of small scale faults, shear zones, minor folds and solution cavities. The maximum height of the cut was 50 m with slope angle of 1V:0.25H, and intermediate benches generally 3 m wide. To control vibrations in the urban neighborhood located nearby and avoid damage to the rockmass, a very cautious and time consuming excavation approach was adopted using rock breakers. The excavation work was completed in 2010. Oman has a hyper-arid environment with scarce rainfall for many months. However, occasionally the area is hit by intense rainstorms. During Cyclone Phet and accompanying rains in June 2010, part of the cut slope failed with a downslope movement of about 800 m^3 of massive rock. This necessitated a post-excavation re-evaluation of the cut slope, which culminated in design modifications, and construction of long term slope stabilization measures that included high capacity rock anchors, rock bolts and reinforced shotcrete for stabilizing potential shallow and deep seated failures. This case history describes the initial design of the cut slope, causes of slope failure during the cyclone, field and laboratory testing carried out for determination of rock engineering parameters, analytical techniques used for design modification and construction details of the designed remedial works.*

KEYWORDS: rock slope, shear strength parameters, Barton Bandis model, limit equilibrium analysis, Shear Strength Reduction (SSR).

SITE LOCATION: IJGCH-database.kmz (requires Google Earth)

PROJECT DESCRIPTION

To provide a shorter connection between the existing Muscat Expressway and a new development in Muscat Municipality, a 6.8 km long ring road traversing through rugged mountainous terrain has been constructed. In order to maintain a convenient grade in the initial 1.5 km, two major box cuts (at RD 0+000 to 0+500 m and 1+120 to 1+480 m) having high and steep cut slopes on either sides were required (Figure 1).

The maximum height of the rock slope in these cuts reaches 50 m with a cut slope of 1V:0.25H (76^o) and 3 m wide benches at every 10 m height interval. A typical section of box cut at RD 0+420 m is shown in Figure 2. The initial design included slope protection measures such as short length rock bolts and reinforced shotcrete.

As the cut slopes were located in the vicinity of commercial and public buildings, the excavation was carried out with mechanical excavators (rock breakers) even though the uniaxial compressive strength of the rock could be as high as 60-80 MPa at places.

A number of rock cuts having similar heights and slope configurations have been constructed in Muscat city and its neighboring wadis (valleys) along many roads and highways. Most of these slopes are unreinforced and only a few are

Submitted: 04 May 2016; Published: 24 March 2017
Reference: Hayat, T.M., Bhatti, T.J. and Goldsmith, R. (2017). *A High Rock Cut Stabilization in Muscat City, Oman*. International Journal of Geoengineering Case histories, http://casehistories.geoengineer.org, Vol.4, Issue 2, p.96-112.
doi: 10.4417/IJGCH-04-02-02

protected with shotcrete. These slopes are generally stable with no history of sliding. Keeping in mind the performance of these slopes, design of the cut slopes at the present site was therefore taken as routine engineering task. However, the conditions at the site were somewhat different than routine and much more challenging. Due to changed and adverse geological conditions at the time of excavation, coupled with intense rainfall due to severe rain events associated with cyclone Phet, a partial failure of the cut slope occured.

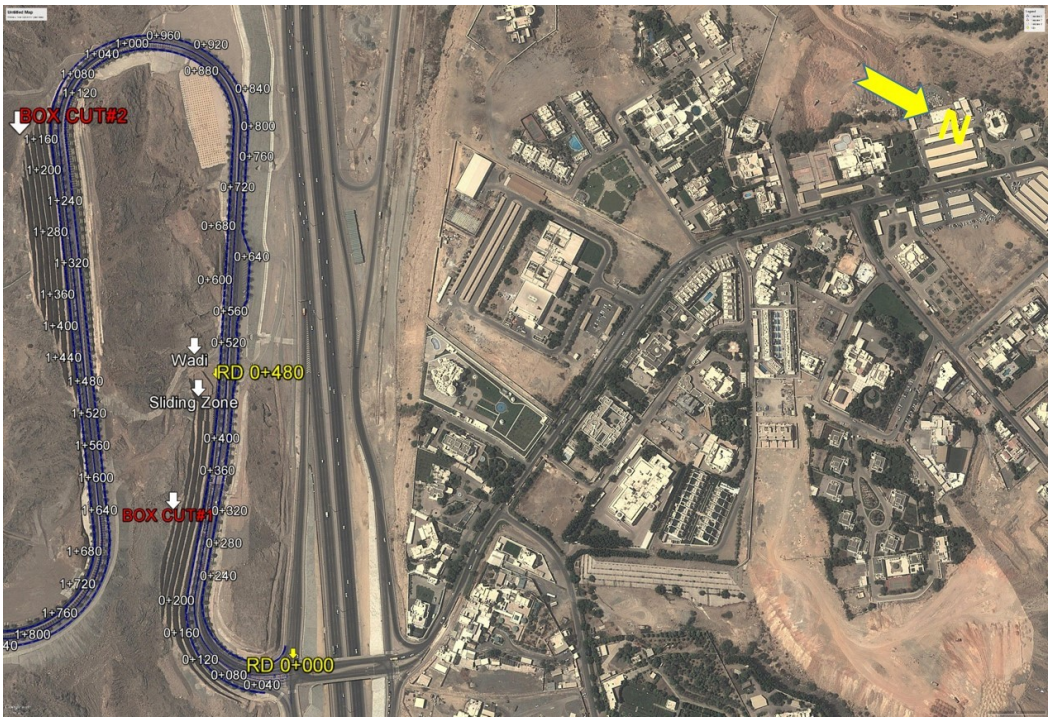


Figure 1. Layout of the Ring Road and its various features of interest to the study identified on Google Earth © Image.

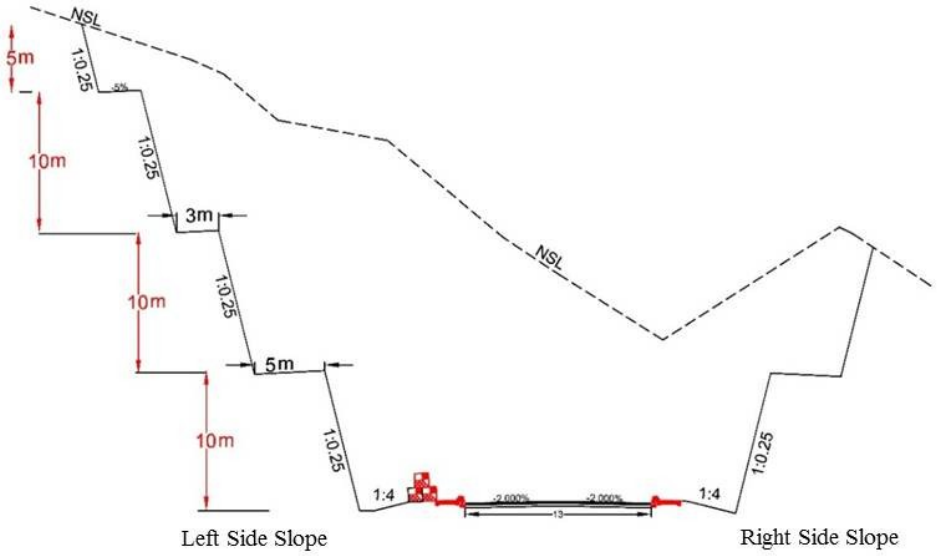


Figure 2. Slope and roadway configuration at station RD 0+420 m in Box Cut#1.

GEOLOGY OF THE AREA

The rocks exposed along the road belong to the Triassic to Jurassic Age Autochthonous Unit "B" sequence of rocks that occupy the coastal ranges behind the city of Muscat. These ranges are foothills extending northeast of Jabal Bawshar. The Autochthonous units were tectonically emplaced along the northeastern edge of the Arabian Platform starting in the late Cretaceous (Villey et.al. 1986). Prior to tectonization, the Triassic to Jurassic calcareous sedimentary rocks were formed in a shallow sea environment. They comprise of dolomite, limestone, fine impure calcareous sedimentary rocks, sandstone, shale and breccias.

The geological sequence is now tectonically stable within the Arabian tectonic plate. The nearest tectonic plate boundaries being the convergence along the Iranian-Pakistani coast, 200 km to the northeast and the Owen Fracture Zone 400-540 km to the east and southeast (Villey et.al. 1986).

Geological Units at the Site

The geological data for the project was obtained from the Geological Map of Síb at a scale of 1:100,000 and the accompanying explanatory notes (Villey et.al. 1986). The rock units at site include, from youngest at the top to oldest at the bottom:

Aruma Group: This consists of siltstone and yellow silty carbonates.

Sahtan Group: This is the younger unit of Jurassic Age and unconformably overlies the Mahil Formation. The Sahtan Group is divided into two separate formations:
Upper Formation (Sa2): Massive blue limestone, decimeter-thick beds are massive, and intensely recrystallised and *Lower Formation (Sa1*): Rust coloured quartzose sandstone alternating with limestone and dolomite, about 20 m thick in the Bawshar area.

Mahil Formation: This is the older unit of Triassic Age. It is a 400-500 m thick sequence also comprising of two members:

Upper Member B: well bedded pinkish-yellow dolomite, with interbedded siltstone and sandstone; and *Lower Member A*: massive beige-grey dolomite, with dolomitic siltstone and thin sedimentary breccias.

An extract of the Sib area geological sheet is shown in Figure 3. It illustrates the geology of Box Cut #1, which consists of ground making a contact between Aruma Group, and Sa2; the Upper Formation of the Sahtan Group. Box Cut #2 follows the contact between Units Sa2 and Sa1.

It is interpreted that the Lower Formation of the Sahtan Group is exposed in Box Cut #1 and the Upper Formation is exposed partly in box Cut #2. There was a discrepancy between the map and what was observed on the ground, i.e. when the built up landmarks were aligned, the geology did not match exactly and vice versa. This could be due to a shift in datum between the1986 map and the project grid. What was observed and mapped on the ground was used in design.

Geological Structure

The geology of foothill range is structurally controlled, striking NE to NNE. The sedimentary sequence, from Triassic to Cretaceous age, appears to consistently dip 20-50 degrees NW to NNW. It is not clear if these are part of large folded structures, but the geological map does indicate some fold plunges along strike with the bedding. It is likely that the bedding is a limb of an anticline fold with its axis SE of the site and trending ENE. Considering the rocks at the box cuts to be a part of a large fold structure there is likely to be intra-formational shearing along the weaker sedimentary layers. Observations at the site indicated that this was indeed the case.
Faults in the area are steeply dipping and generally strike across the bedding trend. This was particularly evident in the box cuts with fault displacements from a few centimeters to several meters. The shear zones did not appear to be wide. The joint pattern also follows steep dip orientations with strikes along WNW-ESE to almost N-S. These appear to be conjugate sets consistent with the strike of the fold axis mentioned earlier.

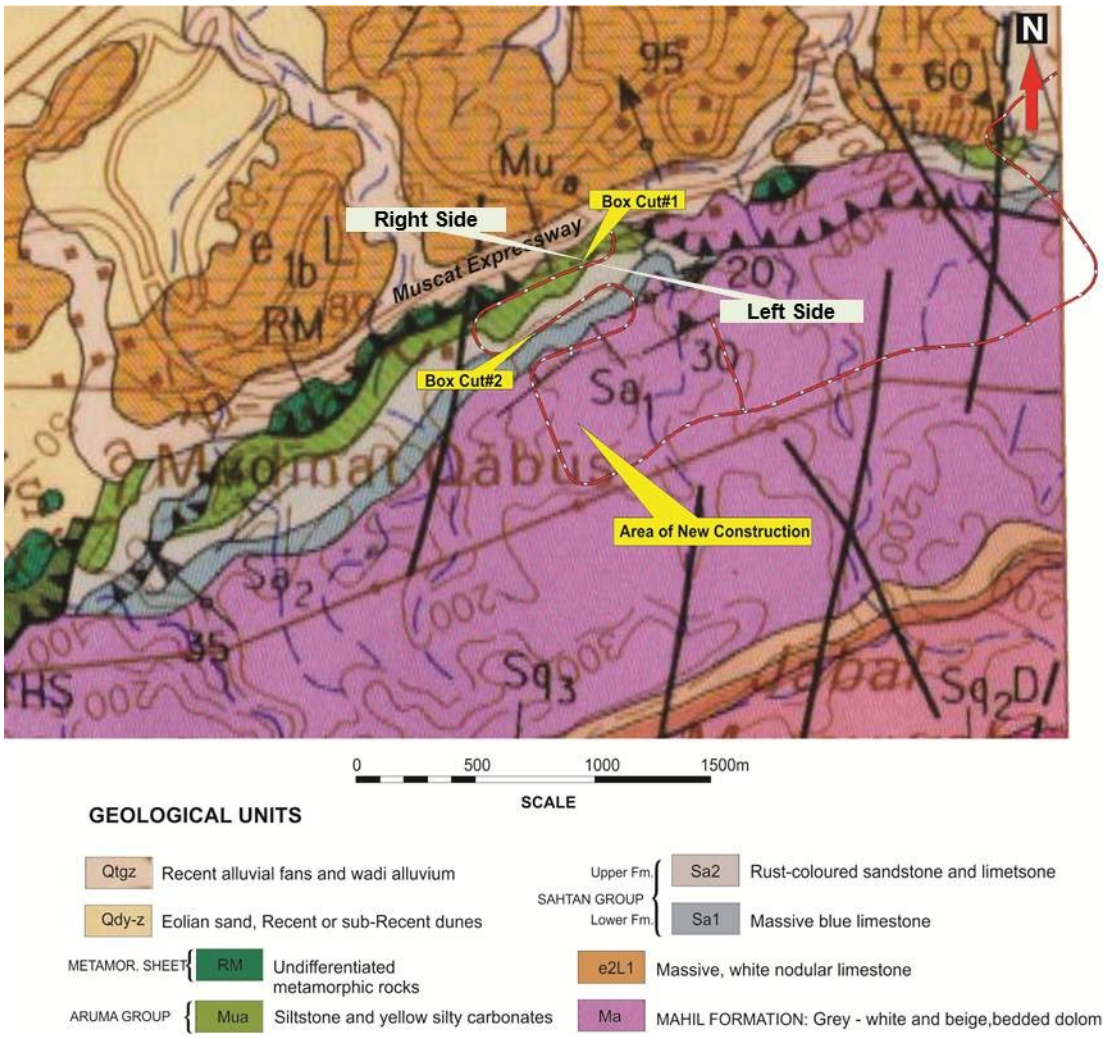


Figure 3. Geological map of the project area.

SLOPE STABILITY ISSUE JUST AFTER CONSTRUCTION

Prior to commencement of excavation, the left slope of Box Cut #1 from RD 0+180 to 0+500 m was envisaged as the most vulnerable area in terms of potential for sliding as the beds in this area of the slope were oriented NE and dip in NW direction at an angle ranging from 30 to 52 degrees with a few being even flatter. The orientation of the bedding joints was, therefore, not favorable as these daylight into the cut slope face, with a potential of a planar type of instability in the rock mass.

Excavation was carried out through mechanical means using rock breakers, therefore no blast induced damage was foreseen or observed. After completion of excavation, most of the cut slopes in the two box cuts generally presented satisfactory profile; however wedge / block failures of small scale were observed along the bench edges and slope faces at numerous locations during walkover inspections, which were carried out prior to the implementation of the designed slope reinforcement and protection measures.

STABILITY ISSUE DURING AND AFTER THE PHET CYCLONE

Oman is generally a hyper-arid region with general scarcity of rainfall, but it has repeatedly been hit by many large tropical cyclones in the past. The Gonu (2007), Phet (2010) and Kaila (2011) storms are recent examples.

After completion of the excavations of the rock cuttings and before the initiation of the proposed slope protection, or stabilization measures, there was an intense rainfall event associated with the Phet cyclone that hit Oman on June 4th 2010.

A rainfall intensity of 55 mm/hour was measured at Mazara Gauging Station about 50 km from the Muscat City with precipitation as high as 450 mm reported at rain gauging stations in northeastern Oman.

This rainfall caused a rock slide on the left side of the Box Cut # 1, from RD 0+380 m to 0+480 m. This section constituted the farthest edge of the cutting. On this side of Box Cut #1, a small wadi (valley) is located behind the slope. This was used as a channel for diverting the storm water from the catchment areas behind the slope. This wadi has steep gradient and was unlined at the time of slope failure.

Photographs taken just after the rain storm showed that the failure had occurred initially as a single event. Failure occurred along a 40^{o} dipping bed in the lowest slope, which extended to the inner edge of the first berm and a near vertical joint forming the release plane. The photographs taken at that time also showed a large amount of water transported debris coming out from the above mentioned wadi adjacent to the failed area. Water was also noticed cascading over the crest of the main rock cut.

With the passage of time, the extent of the initial failure grew in size as more and more rock mass adjacent to the initial failure area failed progressively. Within a couple of weeks of the initial event, the failure grew to the top of the 35 m high cut, extending about 20 m along the crest and reaching as far as a steep joint with a strike of about 260^{o} (N100 deg W), and dip of more than 70^{o}. The total volume of failure was estimated at 800 m^{3} (Figure 4).

From site observations, it was concluded that the failure initiated along a laminated bed of argillaceous rock layers, which had the least shearing resistance of all the rock mass at the site. The failure undermined the slopes above it and caused their failure, which progressed in the weeks ahead of the initial event.

The main triggering factor was the increase in water pressure associated with the rainfall event. The Box Cut # 1 slope at the farthest end was exposed to weather on three sides; the front cut face, the edge face and behind in the wadi (valley). It is likely that the water in the wadi overflowed and infiltrated the loose jointed and bedded rock mass. It is also likely that the small solution channels formed conduits for water that entered the formation, contributing to the failure. Although the rock mass appeared visibly stable in the area after a few weeks, there were other bedding / joints in the area that could cause further instability in the future, especially under wet conditions.

POST FAILURE ANALYSIS AND DESIGN REVIEW

The slope failure indicated that the cut slope design should be revisited and better slope stabilization measures incorporated in the design. Post-failure assessment showed that the site was characterized by alternating beds of competent dolomite/limestone 0.3 to 1 m in thickness, intercalated with more finely laminated argillaceous calcareous rocks (either dolomite or limestone). As indicated above, the two Box Cuts are in different geological units. Box Cut # 1 is in interbedded limestone/dolomite and thin argillaceous units, forming a monotonous sequence over the full height of the excavation. Box Cut # 2 is in more reddish coloured and less laminated dolomite and sandstone or micrite.

In Box Cut #1, from approximately RD 0+220 to 0+500 m, the interlayering of the beds is quite prominent and dips at 30^{o} to 45^{o} daylighting out of the face and within +/- 20^{o} of the face orientation. In addition to the bedding, there are joints and faults that are steeply dipping at 70^{o} to 90^{o} and strike NE-SW or SSW. These joints have high persistence over all cut benches to the full 40 m height. Some of these features are faulted with noticeable displacements. Figure 5 shows the pole plot of the joints and great circles drawn through the centre of poles concentration by visual examination.

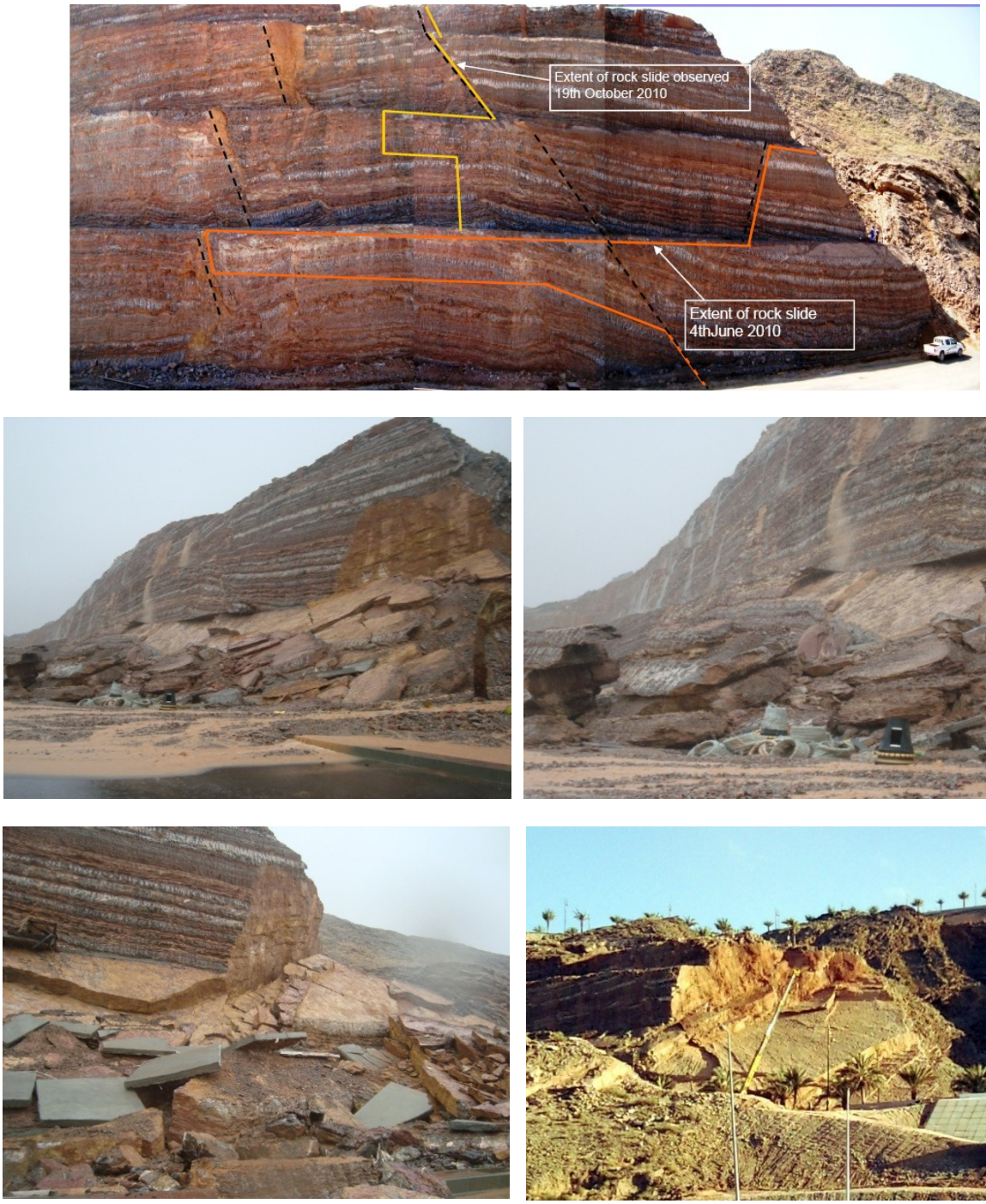


Figure 4. Top photo provides an overall view of the slope face prior to sliding and the extent of two episodes of sliding on June 4th and October 11th 2010. The lower frames, except the lower right corner view, show sliding during Cyclone Phet, while the lower right corner view shows the resulting slope face after the final collapse on October 11th 2010. The sliding along the bedding and a vertical joint, a free release plane along the overspilled wadi, is an obvious reason of sliding during cyclone Phet.

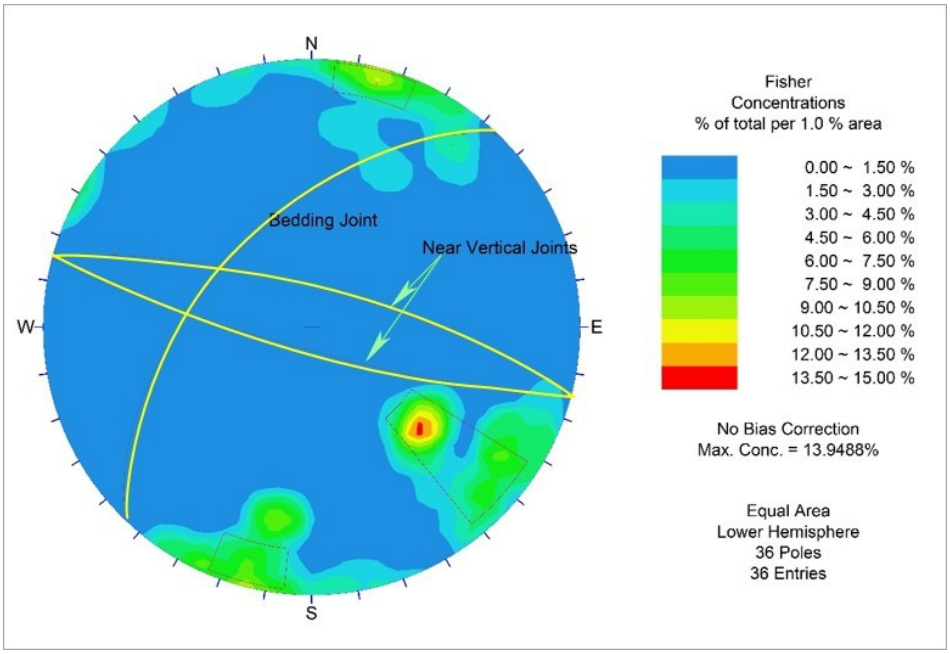


Figure 5. Stereoplot of the discontinuities representing the left slope in Box Cut 1.

The environment in which sedimentary carbonate rocks are formed can be quite variable, from high energy to low energy. Limestone built from coral reefs are formed in a high energy depositional environment and back reef areas are formed in a low energy environment. The high energy areas give rise to bedding surfaces that are highly irregular and undulating and those in the low energy environment are more planar. The more prominent limestone beds in unit Sa2 are likely to have been formed in a moderate energy environment, thus bedding surfaces could be irregular and undulating. This was observed in the rock exposures. Thus, the rock mass at site consisted of competent hard rock beds separated by weak bedding layers that dipped from 25^{o} to 45^{o}. The bedding has measurable undulations and variability that is discussed in the next section.

EVALUATION OF SHEAR STRENGTH OF DISCONTINUITIES

The stability of a rock mass is controlled by the shear strength of its discontinuities, and this project history shows that it was no different in this case either. During the pre-construction analysis, shear parameters were taken optimistically on the higher side, which resulted in minimal slope protection and stabilization measures, such as shotcrete at few locations and rock bolts on benches.
The exposed geology and subsequent failure during cyclone Phet clearly indicated that the shear strength parameters would require revision and re-analysis over the entire project area. It was also clear that water played a major role and had to be accounted for in the re-analysis.

Bandis (1980) and Barton and Bandis (1990) have shown that the shear strength of a rock discontinuity has the following components:

(a) Asperity failure component;
(b) Geometric (dilation) component; and
(c) Residual or basic friction angle component.

The asperity failure component and the geometric component are both scale (block size) dependent (Bandis, 1980) and their values decrease with increasing block size, while the value of residual or basic friction angle is independent of the block size or scale.

Thus an equation could be formulated to represent the above mentioned components of shear strength:

$$\phi = \phi_r + \phi_w + \phi_{JRC} \quad (1)$$

where ϕ_r = Residual or basic friction angle;
ϕ_w = Friction angle due to geometric (waviness) component; and
ϕ_{JRC} = Friction angle due to asperities.

These parameters were then used in the Barton and Bandis (1990) failure criteria as shown below to evaluate the shear strength of rock discontinuity:

$$\tau = \sigma_n tan[\phi_r + \phi_w + \phi_{JRC}] \quad (2)$$

$$\phi_{JRC} = JRC_n Log_{10}(\frac{JCS_n}{\sigma_n})] \quad (3)$$

Substituting for ϕ_{JRC}

$$\tau = \sigma_n tan[\phi_r + \phi_w + JRC_n Log_{10}(\frac{JCS_n}{\sigma_n})] \quad (4)$$

The evaluation of each component was then carried out as explained in the following sections.

The Residual Friction Angle - ϕ_r

Four (4) Hoek shear tests were executed in the laboratory on the calcareous mudstone (calcium-magnesium carbonate with argillaceous minerals). One test was performed on a saw cut surface, while for the other three tests, core samples were manually split into two halves along the cleavage planes and tested.
The results of the Hoek shear tests were:

- Saw cut surface: $\phi = 15.1^o$, c = 50 kPa
- Natural cleavage plane, with undulations: $\phi = 23.2^o$, c = 100 kPa
- Natural cleavage plane, very smooth surface: $\phi = 14.0^o$, c = 180 kPa

It is clear from the tests that the basic friction angle (or equivalent smooth residual friction angle) could be as low as 14^o (ϕ_r). The difference between the friction angle of saw cut smooth surface (15.1^o) and the natural cleavage plane smooth surface (14.0^o) can be attributed to weathering and softening. The saw cut surface is smooth and unweathered, while natural cleavage must have been subjected to various cycles of wetting and drying leading to softening of material and resulting in some reduction in friction angle. Therefore, the value of 14.0^o was adopted for the residual angle and used in analysis.

Friction Angle due to Geometric (Waviness) Component - ϕ_w

The undulations/waviness of a joint surface observed over distances on the order of 1 m to 10 m also contribute by increasing the shear strength of the discontinuity (Miller, 1988). Observations at site related to the shear strength of discontinuities showed that slopes in the surrounding natural rock attained stability at around 30^o to 35^o, indicating that both large scale waviness and asperities were adding to the friction angle.

Hack et. al. (2003) reported that the large scale waviness contributed in increasing the friction angle of a discontinuity. Figure 6 shows the approximate addition to the friction angle that should be incorporated in the design for waviness of various amplitudes in the discontinuities over 1 meter length (Hack et. al. 2003). Miller (1988) reported that the waviness angle could be calculated from the observed variation in the dip of any discontinuity in the field.

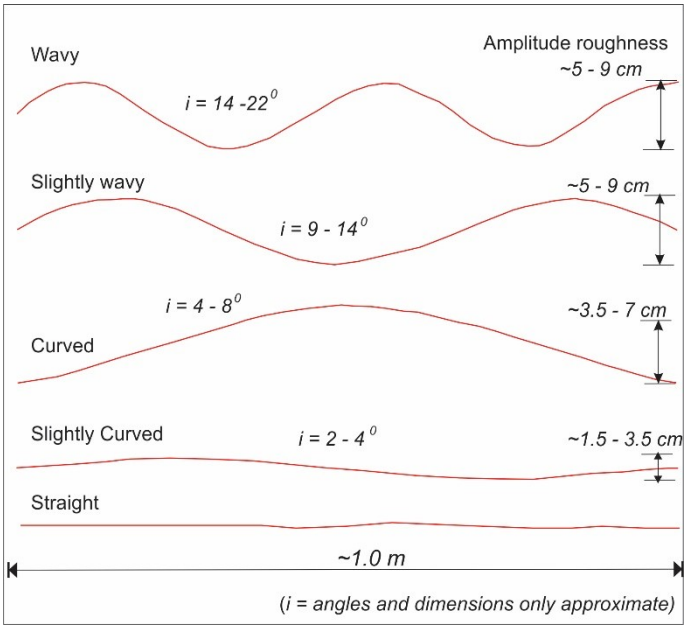


Figure 6. Large scale roughness profiles.

Mapping of the geological structures in both Box Cuts revealed a high degree of variability in waviness. In Box Cut #1 measurements of a single bed over 5.0 m trace length gave a range of dips of 31° to 43°, with a mean of 35°. The dip direction ranged from 315 to 335°. Observations were also made on a smaller scale where there were variations with a general waviness (ϕ_w) that was on the order of $\pm$ 5° over a few meters.

To check the variability in the direction, measurements of dip in some exposures of bedding along the wadi behind Box Cut # 1 at RD 0+500 m were also carried out. The exposed bed near the head of the rockslide indicated a range of dips of 22° to 40° over 5 m dip length.

Other beds that were intact in the rock along the sides of the wadi showed similar characteristics. Thus, both along strike and along dip direction there was variability in structure.
Since the waviness factor is dependent on scale, being lower for longer profiles, 10° waviness angle was selected for small scale failures (small block size) and 5° for deep seated failure planes (large block size), based on site observations of waviness. Thus:

- Single or Double Bench Scale Failures: $\phi_r + \phi_w = 14 + 10 = 24°$;
- Multiple Bench (deep) failures: $\phi_r + \phi_w = 14 + 5 = 19°$;

Friction Angle due to Asperities – ϕ_{JRC}

In the Barton-Bandis (1990) failure criteria, the friction angle due to asperities is calculated by equation 3:

Both the terms JRC (Joint Roughness Coefficient) and JCS (Joint wall Compressive Strength) are dependent on the size of sample. Barton and Bandis (1990) presented a chart that gives the JRC in relation to amplitude of apertures and length of profile.

The JRC value is based on the surface roughness, and amplitude of the discontinuity. Selection of the JRC values between 0 and 20 was quite challenging. The approach used was based on selection of the JRC for a small sample, about 100 mm in length, then modifying the value, either by the chart proposed by Barton or by calculation.

Equation 5 (Barton and Bandis, 1990) relates JRC_o from a small sample to JRC_n for the large insitu condition.

$$JRC_n = JRC_o [\frac{L_n}{L_o}]^{-0.02JRC_o} \quad (5)$$

This equation gives a lower value of JRC_n for the larger scale discontinuity than the JRC_o for bedding joints of 100 mm sample. By comparing the specimen's roughness to the standard roughness profiles recommended by ISRM (1977) the value of 14 was selected. However after applying the scale correction for 10 m block size, the JCR_n comes out 3.9, which was used in calculations.

The JCS is that of the weakest material adjacent to the discontinuity. The initial estimates are generally based on the ISRM methods or by use of the rebound value from a Schmidt hammer. Based on site observations, it is noted that the sedimentary layer materials adjacent to the joint surface were weak and thus a quite low value of 5 MPa was assumed.

Using Equation 4, σ_n-τ plot was developed for 0 to 1200 kPa normal stress levels as shown in Figure 7.
Since, the friction angle is normal stress dependent, the friction angle for any normal stress level was calculated using the relationship given below (Hoek, 2007).

$$\phi_L = arctan\left[\frac{\partial \tau}{\partial \sigma_n}\right] \quad (6)$$

Where, ϕ_L is the friction angle at any given stress level.

Figure 7 shows the spreadsheet results of ϕ_L at various normal stress levels for deep seated failures.

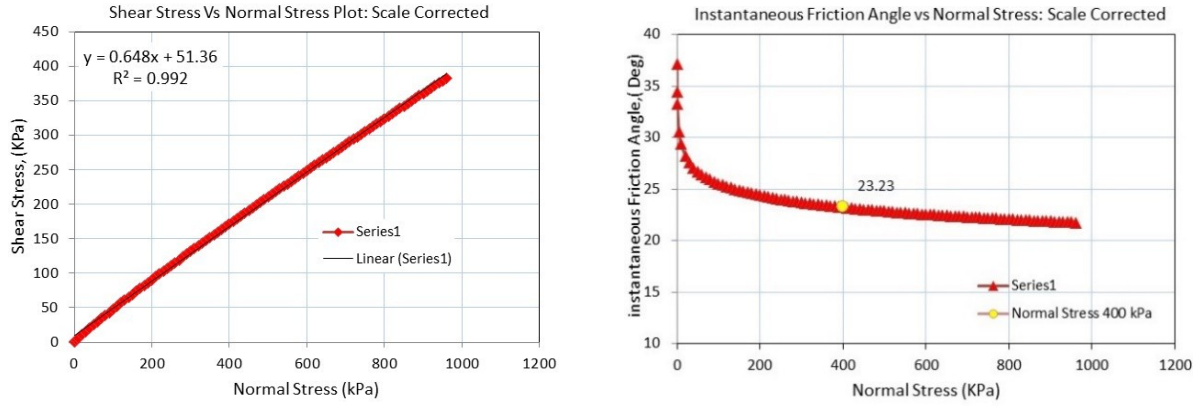


Figure 7. Friction angle at various stress levels for a deep seated sliding plane.

The average normal stress range was found to be about 400 kPa. Considering this, the corresponding friction angle (ϕ_L) was selected as 23.2° from Figure 7. In addition, based on site observations of intact rock bridges and test results, a cohesion value of 80 kPa was selected for analysis in deep seated failures. Similarly, for small scale failure, the ϕ_L value was calculated as 28° and zero cohesion was assumed in this case.

ANALYSIS AND DESIGN OF STABILIZATION MEASURES

Expected Failure Planes

The orientation of bedding planes along various berms showed appreciable variation in the dip inclination. However, previous failures and site observations led to the conclusion that the most likely inclination of the failure plane was 40°. Also smaller scale failures involving one or two benches and larger global scale failures with deep seated planes were both possible. Based on the above, the following expected failure planes were considered in the re-assessment of slope stability:

1. Relatively smaller scale failures involving one or two benches; and

2. Multiple bench (deep) failure (only for the cut slope ends where release surfaces were available for deep sliding and thus failure was kinematically possible).

Figure 8 shows the analyzed failure planes within the rock mass.

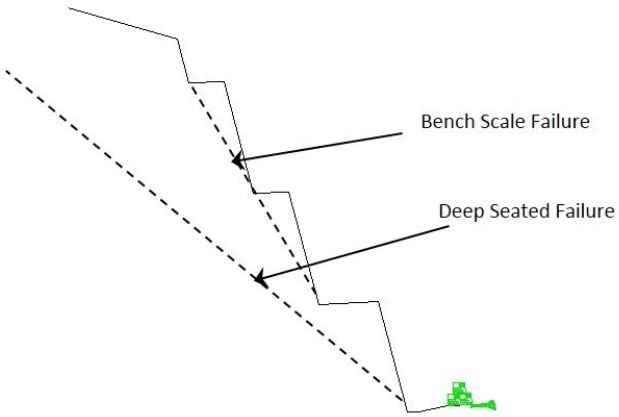


Figure 8. Illustration of relatively small scale and multiple bench (deep) failures planes assumed in stability analysis of Left Face Slope at Km 0+400 m.

A systematic approach was adopted to check the Factor of Safety for single bench, multiple bench and deep seated failures. Presentation of complete results of all these parametric studies is beyond the scope of the paper, however, the results of analysis along the deep seated plane inclined at 40^o is presented. Note that because Oman is located in an aseismic zone (Abdalla and Al. Homoud, 2004), no earthquake loading was considered in the analysis.

Dry Condition Analysis

Hoek & Bray and Bishop Limit Equilibrium Analyses

Hoek & Bray and Limit Equilibrium Analysis (LEA) using Bishop and Morgenstern Price methods were selected to evaluate the Factor of safety of sliding wedge inclined at 40^o, for a 35 m high initially dry slope. ROCPLANE and SLIDE (RocScience Inc., Canada) software were used for the analyses.

The ROCPLANE software uses the traditional Hoek and Bray equation of planar sliding rock wedge (Hoek and Bray 1981), whereas SLIDE takes advantage of splitting the sliding wedge into slices and analyzing the moment and force equilibrium using Bishop or Janbu methods.

Shear Strength Reduction (SSR) Verification

The results of analyses of ROCPLANE and LEA SLIDE were also counter-checked with the Shear Strength Reduction (SSR) Finite Element Method (SSR-FEM) using the RocScience 2D PHASE-2 numeric code.

The SSR technique is used widely by the geomechanics community to model actual stress-strain behavior of the soil/rock. The theoretical background of the approach has been well covered in the literature (Griffith and Lane, 1999, Diederichs et. al., 2007 and Krahn, 2007). The technique is quite straightforward and involves progressive reduction in the shear strength of an elasto-plastic material during analysis until collapse occurs. This collapse situation in the FEA is the point where the system does not converge to satisfy the state of equilibrium and thus an automated SSR (=Factor of Safety) is determined. The mathematical representation of SSR for the Mohr-Coulomb strength parameters is as follows (Diederichs et. al., 2007):

$$C'_{trial} = \frac{1}{FS_{trial}} C'_{measured} \quad (8)$$

$$\emptyset_{trial} = tan^{-1}\left[\frac{1}{FS_{trial}} tan\emptyset\right] \quad (9)$$

$$\tau_{max} = C'^{(i)}_{trial} + \sigma_n tan\emptyset'^{(i)}_{trial} \; for \; the \; i^{th} \; material \quad (10)$$

In the SSR analysis the SRF = FS_{trial}.

For the present study, RocScience PHASE-2 FEM code was used for the SSR analysis. For the purpose of sensitivity analysis, 535 (coarse) and 1821 (fine) six noded triangular elements were used in FE mesh. The ground surface of slope was modeled as a free surface and the rest of the surfaces were assigned with restrains in X and Y directions in the boundary conditions. The shear strength reduction search was limited to the area of the material possessing the lower strength. The same boundary conditions and SSR search approach were used for both the reinforced and unreinforced analyses.

Comparison of Stability Analyses Results

The results of analysis in terms of Factor of Safety for dry slope condition are shown in Table 1 and Figures 9 and 10.

Table 1. Calculated factors of safety along deep seated sliding plane in dry conditions using Hoek & Bray, LEM and FEM methods (With no reinforcement).

Hoek and Bray Method	Bishop Slice (LEM)	Morgenstern-Price (LEM)	FEM -Shear Strength Reduction (SSR)
1.12	1.171	1.174	1.13

From the table above, it is can be observed that the Factors of Safety from the three approaches used are in general agreement. Figure 10 below shows the exaggerated deformed FE mesh of the upper sliding block for the SRF =1.2 (In Dry Condition) for which no FEA convergence occurred.

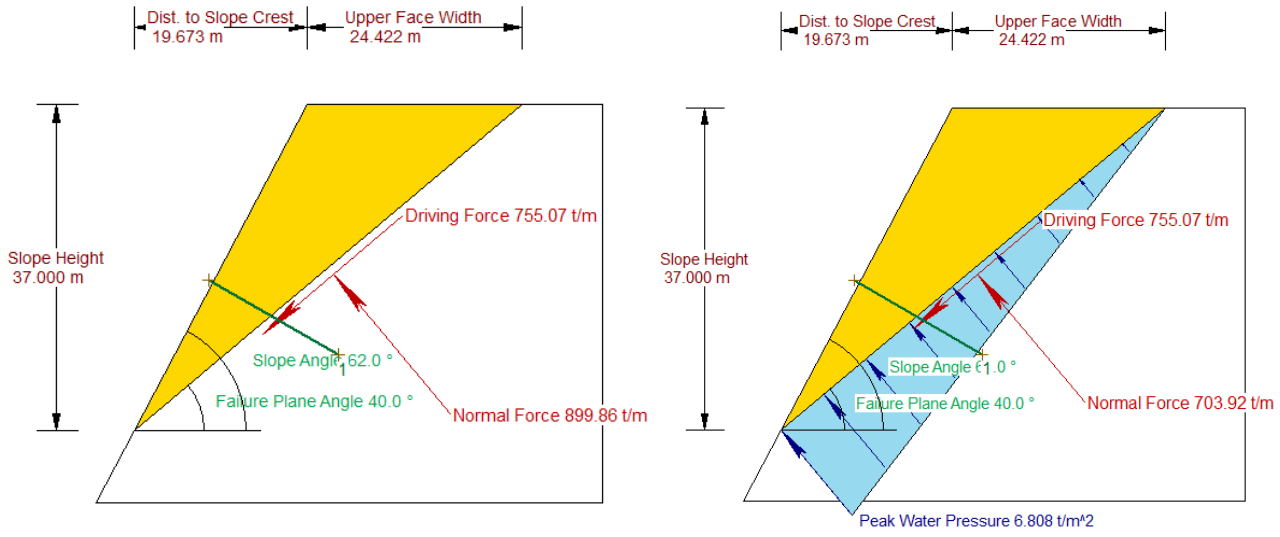


Figure 9. The driving and resisting forces against the calculated FOS 1.12 and 1.01 for dry and wet slope (15 m water head) respectively.

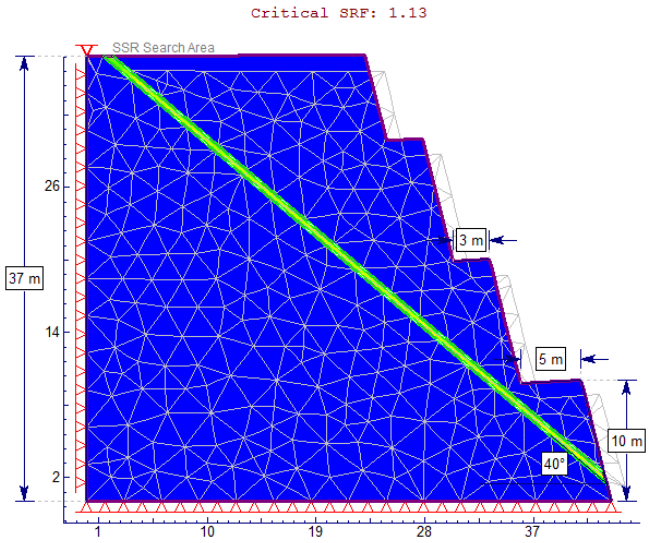


Figure 10. Deformed mesh for the SRF =1.2 (in dry conditions) for which no FEA convergence occurs. The maximum SRF for which the FEA satisfies the state of equilibrium is 1.13.

MODELLING THE WATER PRESSURE

It was also considered that conditions similar to that of cyclone Phet could reoccur during the service life of the project, and thus the stability of cut slopes required evaluation under wet conditions.

The limestone and dolomite beds of host rock were found to be extremely strong and non-fractured. Therefore a uniform groundwater or phreatic line was unlikely to develop in these. It was envisaged that the possible seepage paths would be in the soft calcareous mudstone joints/beds. Thus water pressures equivalent to 15, 18 and 22 m static water head was applied on the 40^{o} inclined failure plane of 35 meter high slope (Figure 8). Different water head values were applied as part of a parametric study to gauge the water pressure that may have acted on the slope when part of it failed.

In analyses, the peak water pressure at the toe was applied in view of adopting a conservative approach as the mid-height water pressure gives slightly higher FOS under similar static water head and material strength conditions. Figure 9 above gives a graphical representation of applied water pressure along the sliding plane.

The results of analysis with water pressure are shown in Table 2.

Table 2. Parametric factors of safety in wet conditions using Hoek and Bray Method (No Reinforcement).

FOS at Water Pressure Eq. to 15 m Static Head	FOS at Water Pressure Eq. to 18 m Static Head	FOS at Water Pressure Eq. to 22 m Static Head
1.01	0.98	0.90

Based on the analyses, it was concluded that the sliding of June 2010 during Cyclone Phet resulted from low shear strength along argillaceous rock joints and water pressure equivalent to 15 m of water head acting on the slide plane. This pressure was then used in the design of slope reinforcement. It was further anticipated that the installation of weep holes in shotcrete and deep drainage holes in rockmass will allow for the joint water pressure to remain below 15 m head. Additionally, the

concreting of benches and diversion of rain water through reverse slope benching will not permit the water to flood the slope faces.

SLOPE REINFORCEMENT FOR STABILIZATION

Realizing the extreme importance of the route and assured road safety for the commuters, a Factor of Safety more than 1.5 in static condition was an essential requirement for slope stability. The slope stabilization measures were modeled in the ROCPLANE software (RocScience Inc., Canada) and other design approaches mentioned above were used to cross check the results.

After several trials using different applied normal stresses on the failure plane, seven strand anchors of 1200 KN working load at 2.5 x 2.5 m grid (3400 KN/m) for a 35 m high slope were selected. The results of factor of safety using the 1200 KN anchors on the deep sliding planes are presented in Figures 11 to 14 and are summarized in Table 3.

Table 3. Factors of safety for deep seated failure plane with seven cable anchors of 1200 KN (2.5 x 2.5 m gird).

Hoek and Bray Dry (Wet at 15 m Head)	Limit Equilibrium Bishop (Dry)	Limit Equilibrium Morgenstern Price (Dry)	FEM -Shear Strength Reduction -SSR (Dry)
1.61 (*1.5*)	1.9	1.7	1.66

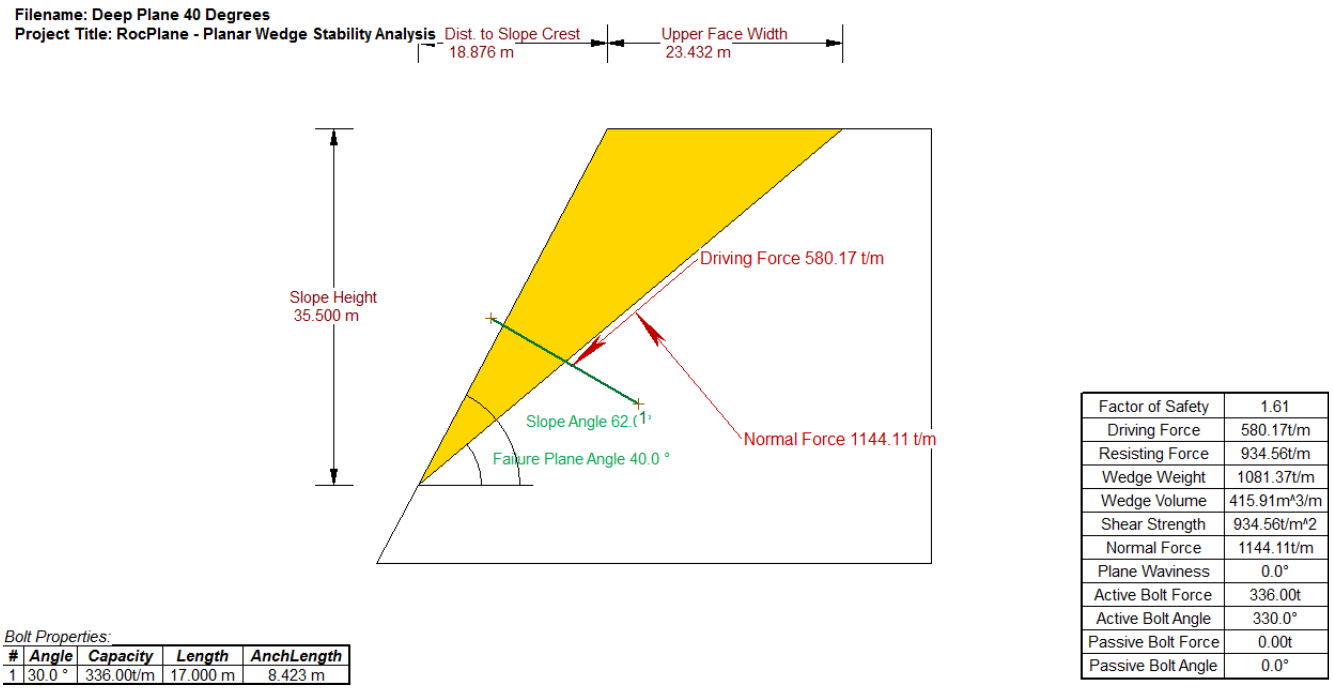


Figure 11. Factor of Safety (FOS) in dry condition with 3360 KN/m external force applied through designed cable anchors.

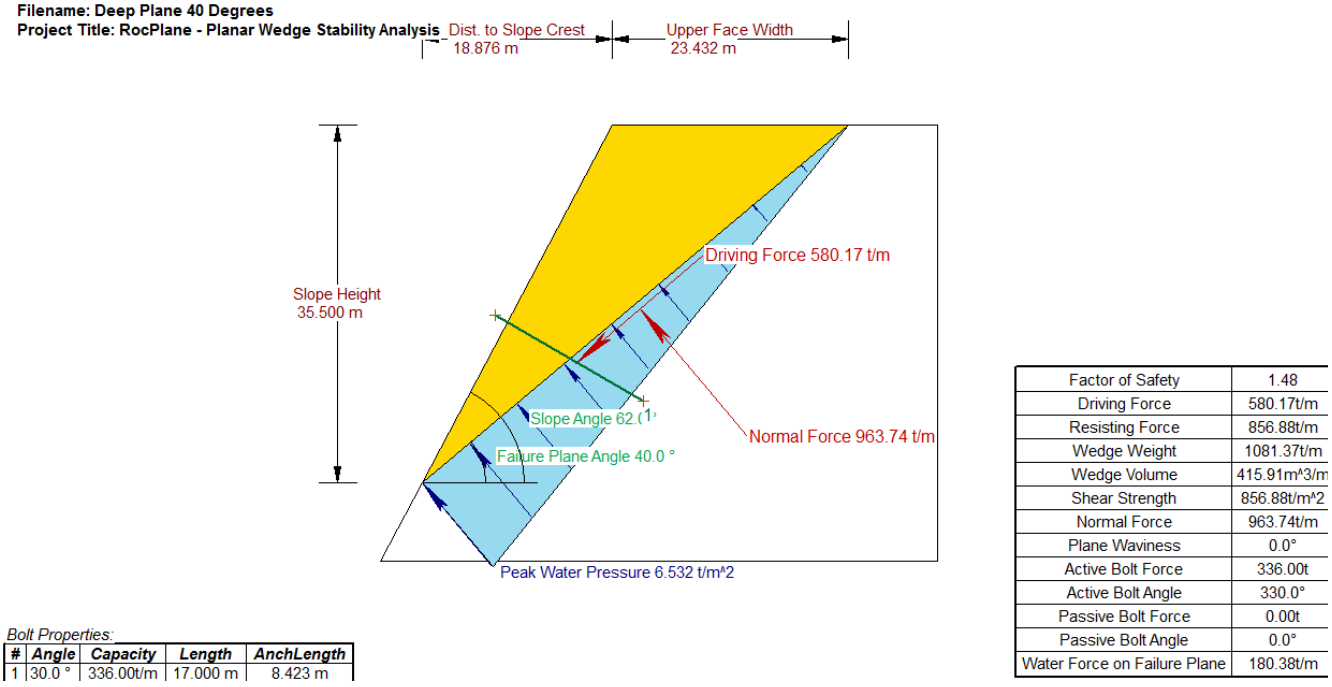


Figure 12. Factor of Safety (FOS) in wet condition under 15 m water head and 3360 KN/m external force applied through designed cable anchors.

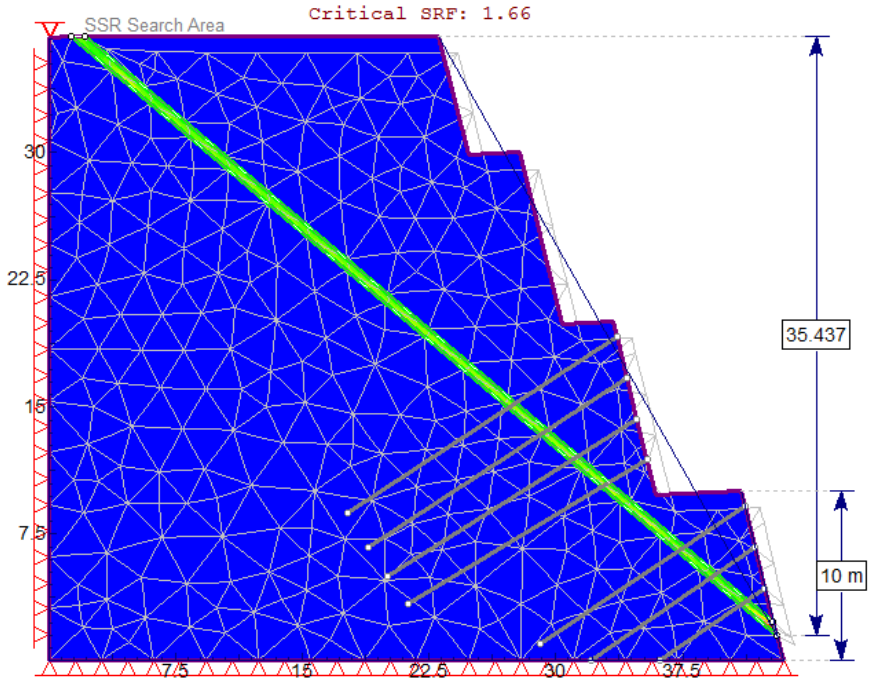


Figure 13. Deformed Mesh for the SRF =1.72 (in dry conditions) for which no FEA convergence occurred. The critical SRF for which the FEA satisfied the condition of equilibrium with 7 strand anchors of 1200 KN (2.5 x 2.5 m grid) is 1.66 as shown.

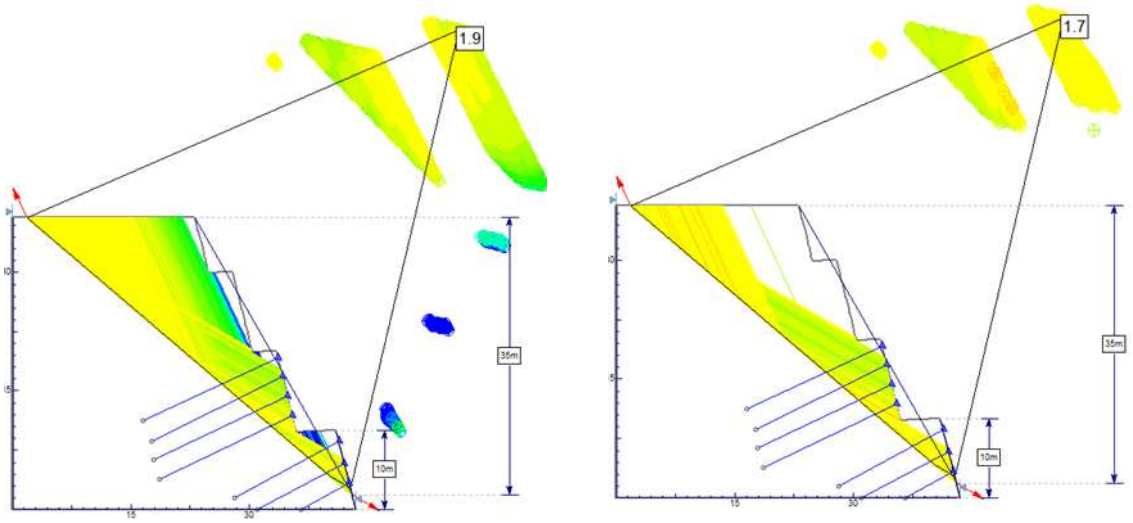


Figure 14. FOS with 7 x 1200 KN anchors in dry condition using Bishop (left) and Morgenstern-Price (right) methods.

VALUE ENGINEERING FOR REINFORCEMENT

Economizing the stabilization measures was also considered during the design re-evaluation. To develop a true planar failure, one of the required conditions is the presence of free release surfaces on either side of the sliding block. The slide of June 2010 was a typical example of this condition. The lack of confinement on the wadi side provided one of the free release planes, whereas persistent vertical joints provided the second release plane.

It was therefore concluded that the ends of box cut #1 were most vulnerable as at these locations large and deep seated failures were kinematically possible, whereas in the middle of these slopes, only shallower failures would be possible, the unstable wedges being confined at both ends. It was therefore decided to reinforce only the terminus of the 500 m long vulnerable slope with 1200 KN cable anchors. Other intermediate and cut faces above the cable anchored slopes were, however, reinforced with 200 KN rock bolts to control the comparatively smaller scale failures. The rock bolt heads were tensioned on steel plates resting on epoxy cement base. For long term durability, the steel plates were embedded in the shotcrete. The anchor heads of high capacity cable anchors were installed on specially constructed reinforced concrete anchor blocks. A typical arrangement of the reinforcement pattern at cut slope ends is shown in Figure 15.

The arrangement of stabilization measures shown in Fig. 15 were implemented and are performing satisfactorily for the last six years.

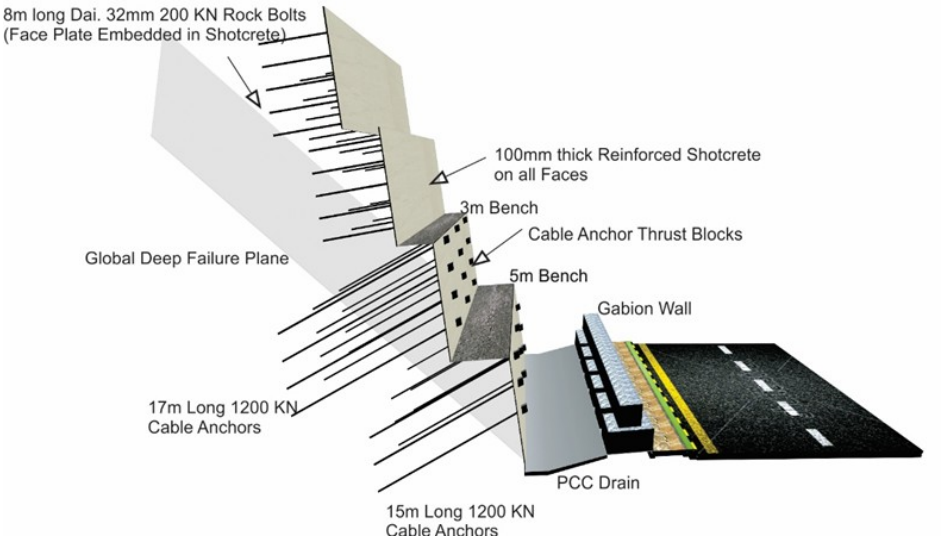


Figure 15. 3D Conceptual arrangement of reinforcing elements at both the 20 m terminus of 500 m long left slope of Box Cut #1.

CONCLUSIONS

This case history had many challenges from which lessons were learned. The following were the main conclusions:

1. The pre-excavation design was based on over-optimistic estimation of the condition and strength of rock.
2. Inadequate drainage arrangements contributed to the failure.
3. It is imperative that geologists/geotechnical engineers are present in such projects so that they can observe changed conditions than those envisaged in design and raise flags so that timely design changes can be incorporated, otherwise the outcome could be slope failures with drastic consequences.
4. The selection of shear strength parameters for rock discontinuities is both a science and an art. It involves combining experience and judgment with laboratory tests and site investigations plus keen observations. For the present case study the methodology adopted was based on combining experience and judgment with site observations and laboratory test results. The present methodology shows promise of application in other projects of similar nature, where time and budget has to be balanced.
5. The Hoek and Bray, Bishop and Morgenstern - Price, and FEA- Shear Strength Reduction (FEA-SSR) approaches were used for calculating the Factor of Safety (FOS) and gave comparable results, with a slightly higher FOS in case of Limit Equilibrium Method.
6. The overall cost of slope reinforcement can be curtailed considering the global slope geometry and kinematics of possible slope failures.

REFERENCES

Abdalla, J. A. and Al. Homoud, A. (2004). "Earthquake Hazard Zonation of Eastern Arabia." *13th World Conference on Earthquake Engineering*, Vancouver, B.C., Canada.

Barton, N. R. and Bandis, S. C. (1982). "Effects of block size on the shear behavior of jointed rock." *Proc. 23rd U.S. Symposium on Rock Mechanics*, Berkeley, USA, 739-760.

Barton, N. R. and Bandis, S. C. (1990). "Review of predictive capabilities of JRC-JCS modeling in engineering practice." In Barton, N and Stephansson, O (eds). *Proc. of the International Symposium on Rock Joints*, Loen, Norway. Balkema, 603-610.

Diederichs, M. S., Lato. M., Hammah, R., and Quinn, P. (2007). "Shear Strength Reduction Approach for Slope Stability Analyses." *Proc. of the Ist Canada-US Rock Mech. Symposium*, Vancouver, Canada.

Griffith, D. V., and Lane P. A. (1999). "Slope Stability Analysis by Finite Elements." *Geotechnique, 49*(3), 387-403.

Hack, H. R. G. K., Price, D. G. and Rengers, N. (2003). "A new approach to rock slope stability: A probability classification SSPC." *Bulletin of Engineering Geology and the Environment IAEG*, 62, 167-184.

Hoek, E., and Bray, J. W. (1981). *Rock Slope Engineering, Institute of Mining and Metallurgy*, Taylor & Francis, London.

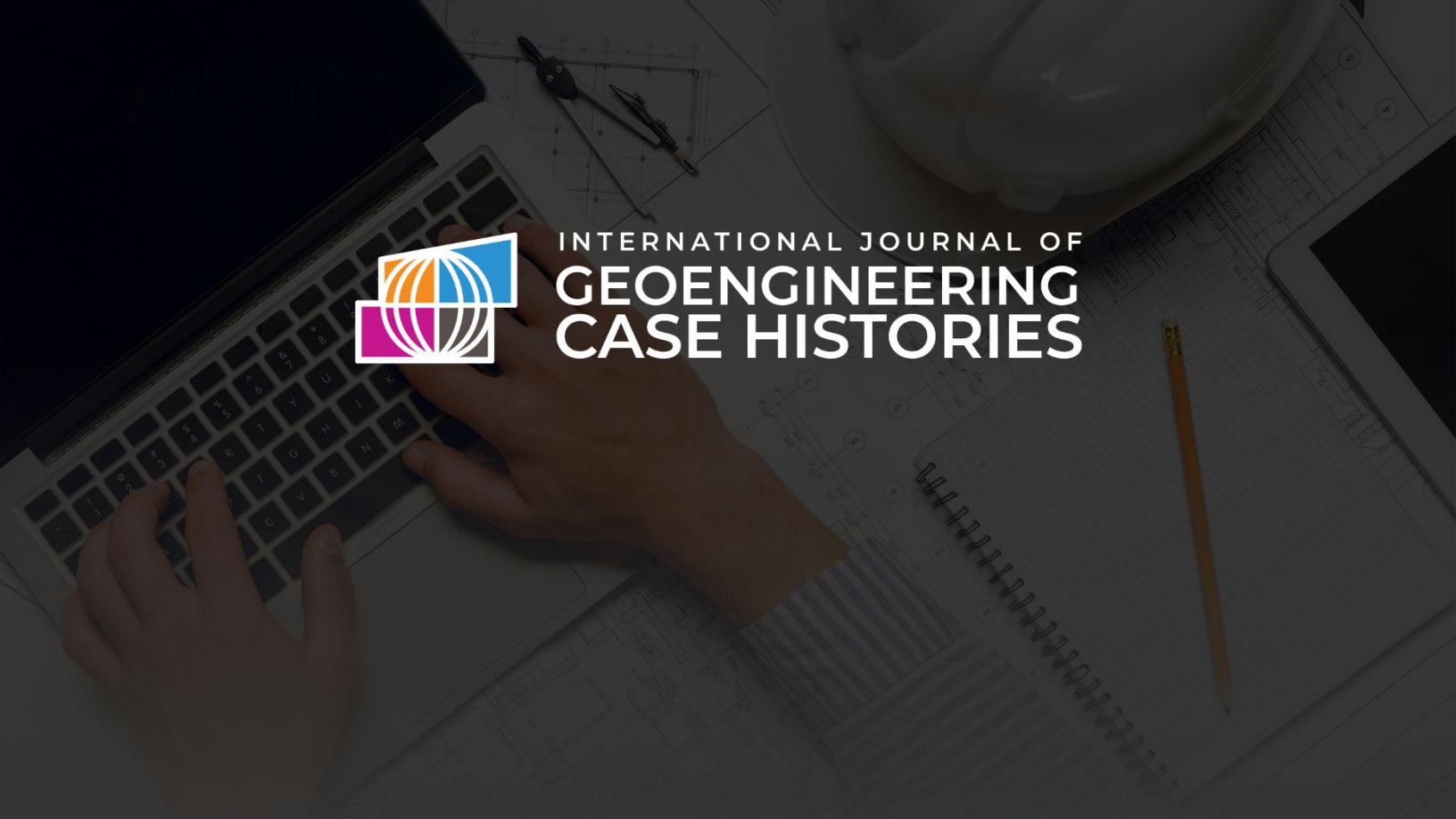
Hoek E.(2007). "Practical Rock Engineering.", Rocscience,<https://www.rocscience.com/documents/hoek/corner/Practical-Rock-Engineering-Full-Text.pdf>

International Society for Rock Mechanics, (1977). *Rock Characterization Testing and Monitoring- Suggested Methods*, Edited by E. T. Brown

Miller, S. M. (1988). "Modeling Shear Strength at Low Normal Stresses for Enhanced Rock Slope Engineering." *Proc. of 39th Highway Geology Symposium*, 346-356.

National Engineering Services Pakistan (2011). *Report on Protection and Stabilization of Cut Slopes – Phase 1*, Issued to the Royal Office, Sultanate of Oman.

Villey, M. de Gramont X and Le Metour, J. (1986). "Explanatory Notes, Geological Map of Síb, Sultanate of Oman." Sheet NF 40 – 3C; Scale 1:100,000. Prepared by BRGM, France.



INTERNATIONAL JOURNAL OF
GEOENGINEERING
CASE HISTORIES

The Journal's Open Access Mission is generously supported by the following Organizations:

dar
a Sidara company

Geosyntec consultants
engineers | scientists | innovators

CONETEC
MUD BAY DRILLING
LANKELMA
Geotech DRILLING

ENGEO
Expect Excellence

Access the content of the ĪSSMGE Īnternational Journal of Geoengineering Case Histories at:
www.geocasehistoriesjournal.org

Downloaded: Thursday, November 19 2026, 08:40:27 UTC